Electronic Dispersion Anomalies in Iron Pnictide Superconductors

Andreas Heimes,[1,4] Roland Grein,[1,2] and Matthias Eschrig[1,2,3,4]

[1]*Institut für Theoretische Festkörperphysik, Karlsruhe Institute of Technology, D-76131 Karlsruhe, Germany*
[2]*DFG-Center for Functional Nanostructures, Karlsruhe Institute of Technology, D-76128 Karlsruhe, Germany*
[3]*Fachbereich Physik, Universität Konstanz, D-78457 Konstanz, Germany*
[4]*SEPnet and Hubbard Theory Consortium, Department of Physics, Royal Holloway, University of London, Egham, Surrey TW20 0EX, United Kingdom*

(Received 20 October 2010; published 25 January 2011)

Recently, experimental studies of the spin excitation spectrum revealed a strong temperature dependence in the normal state and a resonance feature in the superconducting state of several Fe-based superconductors. Based on these findings, we develop a model of electrons interacting with a temperature dependent magnetic excitation spectrum and apply it to angle resolved photoemission in $Ba_{1-x}K_xFe_2As_2$. We reproduce in quantitative agreement with experiment a renormalization of the quasiparticle dispersion both in the normal and the superconducting state, and the dependence of the quasiparticle linewidth on binding energy. We estimate the strength of the coupling between electronic and spin excitations. Our findings support a dominantly magnetic pairing mechanism.

DOI: 10.1103/PhysRevLett.106.047003 PACS numbers: 74.70.Xa, 74.20.Pq, 74.25.Jb, 78.70.Nx

Shortly after the discovery of high-temperature superconductivity in Fe-based pnictide compounds [1] a magnetic Cooper-pairing mechanism was proposed [2,3], while electron-phonon interaction as primary pairing mechanism was found to be unlikely [4]. This conjecture is supported by the proximity of antiferromagnetism and superconductivity in the phase diagram [5,6]. The spin excitation spectrum of pnictides shows pronounced similarities with other superconductors where a magnetic pairing mechanism is under debate. In particular, the strong temperature dependence of the normal state spin excitations studied recently by Inosov *et al.* [7], as well as the presence of a spin resonance feature in the superconducting state [8] are prominent features also present in cuprates and in some heavy fermion superconductors.

Angle resolved photoemission (ARPES) measurements reveal a sharp Fermi surface consisting of electronlike and holelike pockets that exhibit comparable superconducting order parameter amplitudes and are nearly nested by the antiferromagnetic wave vector $\boldsymbol{Q}$ [9,10], a reason to believe that magnetic and electronic order are closely connected [11]. This raises the question how strongly electrons couple to spin fluctuations, as those lead to an effective electron-electron attraction, if the order parameter changes the sign on the different pockets [12]. Investigating the low-energy dispersion anomalies, whose position and shape can be traced back to a coupling of bosonic modes, has proven to be a powerful method for obtaining this information [13–15]. Recent experimental studies on the superconducting state spectral function of $Ba_{1-x}K_xFe_2As_2$ measured by ARPES find such an anomaly, which appears as a kink in the dispersion relation at about 25 meV [15]. On the other hand, inelastic neutron scattering (INS) studies of this compound reveal the development of a resonant spin excitation in the superconducting state [8]. The temperature dependence of both neutron intensity and the self-energies extracted from ARPES follow an order parameter like evolution. This strongly indicates that the spin resonance indeed accounts for the observed anomaly.

Below, we present a theoretical model that explains the anomalous features in the dispersion relation by a coupling of electrons to a spin-fluctuation spectrum that (a) reproduces the experimentally observed temperature dependent spectrum in the normal state and (b) features a low-energy resonance in the superconducting state. We show that coupling to such a spin-fluctuation spectrum leads to a renormalization of the quasiparticle dispersion even in the normal state and can account for the renormalization factor necessary to project density functional theory (DFT) calculations to experiment. Furthermore, we are able to quantitatively reproduce experimental ARPES results, including low-energy and high-energy renormalization of the dispersion and the energy dependence of the quasiparticle linewidth.

Spin-fluctuation spectrum.—Although there are various theoretical models for the spin-spin response function, here we prefer a semiphenomenological approach, taking the spin susceptibility from experiment. This approach was very successful in the case of cuprates [13], and has the advantage of being independent of a specific theoretical model for explaining the origin of the magnetic resonance.

A detailed investigation of the spin dynamics in the normal state and the temperature dependence of the spin resonance in pnictides was recently performed on optimally doped $BaFe_{1.85}Co_{0.15}As_2$ by Inosov *et al.* [7]. They observe that the imaginary part of the normal state susceptibility near the antiferromagnetic wave vectors $\boldsymbol{Q}_\alpha$ obeys in good approximation the Ornstein-Zernicke form

$$\chi_n^c(\omega, \boldsymbol{q}) = \sum_{\alpha=1,2} \frac{b_{n,\alpha}\chi_T}{1 + \xi_T^2|\boldsymbol{q} - \boldsymbol{Q}_\alpha|^2 - \imath(\omega/\Omega_{\max}^T)}, \quad (1)$$

where $\chi_T = \chi_0/(T + \theta)$ controls the strength of magnetic correlations, $\Omega_{\max}^T = \Omega_0(T + \theta)$ sets the typical spin-fluctuation energy scale, $\xi_T = \xi_0/\sqrt{T + \theta}$ is the magnetic correlation length and θ is the Curie-Weiss temperature. The orbital index n will be discussed below.

With decreasing temperature spectral weight is shifted towards lower energies. Below T_c the spectrum becomes gapped and a resonance appears at an energy that follows approximately an order parameter like evolution, i.e. $\Omega_{\rm res}^T = \Omega_r\sqrt{1 - T/T_c}$. In order to model the resonance below the quasiparticle continuum we assume a (sharply peaked) Lorentzian in energy and a separable form for the momentum dependence,

$$\chi_n^r(\omega, \boldsymbol{q}) = \sum_{\alpha=1,2} \frac{2\Omega_{\rm res}^T/\pi}{(\Omega_{\rm res}^T)^2 - (\omega + \imath\Gamma_{\rm res})^2} \frac{b_{n,\alpha}w_T}{1 + \xi_r^2|\boldsymbol{q} - \boldsymbol{Q}_\alpha|^2}. \quad (2)$$

We approximate the gapped continuum in the superconducting state for ω above a temperature dependent continuum threshold, $\omega > 2\bar{\Delta}(T)$, by its normal state value, Eq. (1), at the respective temperature. Here, $\bar{\Delta}$ is the mean superconducting gap at the nested Fermi surfaces. Thus, we model the imaginary part of the complex dynamical susceptibility by $\chi_n''^{\rm sc}(|\omega| < 2\bar{\Delta}) = \chi_n''^r$ and $\chi_n''^{\rm sc}(|\omega| \geq 2\bar{\Delta}) = \chi_n''^c$, and calculate the real part by exploiting Kramers-Kronig relations. We note that this approximation is excellent except possibly close to the continuum threshold. The resonance weight-factor w_T in Eq. (2) is determined by a local sum rule which fixes the ratio between resonance and continuum, w_T/χ_T [16]. It is chosen so that the energy and momentum integrated spin structure factor, $\int_{-\infty}^{\infty} d\omega \int d\boldsymbol{q} S(\boldsymbol{q}, \omega)$, with $S(\boldsymbol{q}, \omega) = 2\hbar\chi''(\boldsymbol{q}, \omega)/(1 - e^{-\hbar\omega/k_BT})$ remains temperature independent below, across, and above T_c.

The overall weight χ_0 enters our theory only in combination with the coupling constant g, and hence only the quantity $g^2\chi_0$ can be inferred from it. A value of g can be obtained if experimental values of χ_0 are available.

In order to take care of the periodicity in reciprocal space we replace the factors $|\boldsymbol{q} - \boldsymbol{Q}_\alpha|^2$ in Eqs. (1) and (2) by $4[\sin^2(\frac{q_x - Q_{\alpha x}}{2}) + \sin^2(\frac{q_y - Q_{\alpha y}}{2})]$, and we neglect the dependence on q_z for our purpose as it varies weakly [17]. We use as length unit the lattice constant a. The resulting momentum dependence at the resonance energy is shown in Fig. 1(a), with the two antiferromagnetic wave vectors $\boldsymbol{Q}_1 = (\pi, 0)$ and $\boldsymbol{Q}_2 = (0, \pi)$. These wave vectors connect Fermi surface sheets with same orbital character ($n = 1, 2, \ldots, 5$ corresponding to the five Fe orbitals d_{xz}, d_{yz}, $d_{x^2-y^2}$, d_{xy}, $d_{3z^2-r^2}$), as illustrated in Fig. 1(a). Here, we consider only the main orbital contributions to quasiparticle scattering resulting from the $n = 1$, 2, 4 orbitals and describe the different momentum variations with the help of the parameter $b_{n,\alpha}$ ($= 1/2$ for $n\alpha = 11$, 22, 41, 42, and $= 0$ else). To obtain the band structure, we employ the tight-binding fit in orbital basis of Ref. [18], which is based on the DFT band structure of $BaFe_2As_2$. In Fig. 1(a) we show the bare Fermi surface for $k_z = 0$, corresponding to 1 Fe/unit cell. The hole pockets at $(0, 0, k_z)$ and (π, π, k_z) are nearly nested to the electron pockets at $(0, \pi, k_z)$ and $(\pi, 0, k_z)$ by the wave vectors $\boldsymbol{Q}_1$ and $\boldsymbol{Q}_2$[18–20].

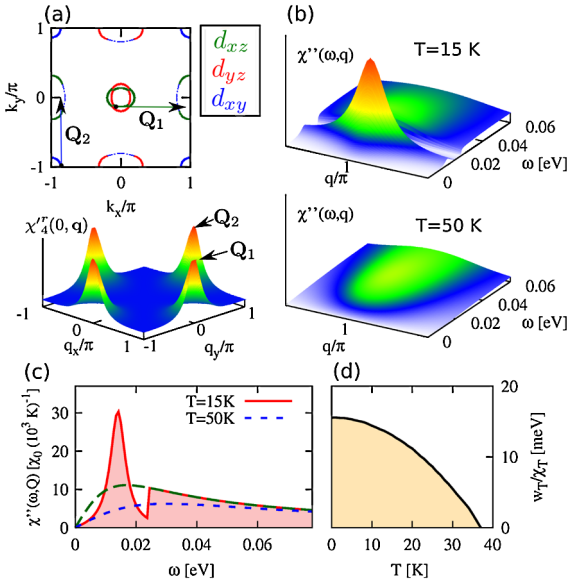

FIG. 1 (color online). (a) Dominant orbital contributions at the $k_z = 0$ Fermi surface cut (top); momentum dependence of the spin-fluctuation mode (bottom). The mode is centered at wave-vectors $\pm\boldsymbol{Q}_1 = (0, \pm\pi)$ and $\pm\boldsymbol{Q}_2 = (\pm\pi, 0)$. (b) Energy-momentum dependence of the spin susceptibility in the normal state ($T = 50$ K, bottom) and in the superconducting state ($T = 15$ K, top). (c) Spectral function $\chi''(\omega, \boldsymbol{Q})$ for $T = 50$ K (dotted) and $T = 15$ K (solid). The dashed line shows the behavior for $T = 15$ K if the material were in the normal state. (d) The ratio w_T/χ_T as function of temperature.

We apply this model to hole-doped $Ba_{0.6}K_{0.4}Fe_2As_2$, where data are available for spin and electronic excitations as well as angle resolved photoemission. In Fig. 1 the momentum and energy dependence for the parameter set $w_{T=0\,\rm K}/\chi_{T=0\,\rm K} = 15.6$ meV, $\Omega_0 = 0.375$ meV/K, $\xi_0 = 5.84$ K$^{1/2}$, $\theta = 30$ K, $\xi_r = 2$, $\Omega_r = 15.5$ meV, $\Gamma_{\rm res} = 3$ meV is presented. The resonance in the spin excitation appears at an energy $\Omega_{\rm res}^{T=7\,\rm K} \approx 14$ meV [8]. In momentum space the mode is peaked around the wave vectors $\boldsymbol{Q}_1 = (\pi, 0, q_z)$ and $\boldsymbol{Q}_2 = (0, \pi, q_z)$ with correlation length ξ_r of nearly twice the lattice constant [Fig. 1(a)]. Comparing the energy-momentum distribution in the normal and the superconducting state [Fig. 1(b) and 1(c)], we see that low-energy spectral weight is shifted into the resonance when the continuum gap opens below $2\bar{\Delta}$. In addition, the sharpened momentum distribution leads to an enhancement of the resonance intensity. In Fig. 1(d) we show the numerically calculated ratio w_T/χ_T, which features this evolution and is in excellent agreement with the functional form $w_T/\chi_T = w_{T=0\,\rm K}/\chi_{T=0\,\rm K}(1 - T^2/T_c^2)$.

Coupling to spin fluctuations.—We are interested in the renormalization of the fermionic dispersion as a result of

the coupling of electrons to the spin-fluctuation mode. For this we numerically determine the electronic spectral function $A(\epsilon, \boldsymbol{k}) = -\frac{1}{\pi}\,\mathrm{Im}(\sum_m[\hat{G}^R_{mm}(\epsilon, \boldsymbol{k})]_{11})$. The Nambu-Gor'kov Green's function $\hat{G}_{mp}(\epsilon, \boldsymbol{k})$, with orbital indices m and p, fulfills the Dyson-equation $\hat{G}_{mp} = \hat{G}^0_{mp} + \sum_n \hat{G}_{mn}[-\frac{i}{2}g^2\chi_n * \hat{G}^0_{nn}]\hat{G}^0_{np}$, with the bare Green's function $\hat{G}^0_{mp}$, the susceptibility χ_n taken from Eqs. (1) and (2) and the coupling constant g, which is assumed to be independent of energy, momentum and orbital number [16]. The idea is to extract the influence of the resonance by comparing the superconducting and normal state dispersion from which self-energy effects are directly inferred. This allows for an immediate comparison with experiment.

Dispersions obtained from ARPES usually differ from DFT calculations by a renormalization factor of 2 [21,22]. In the upper panel of Fig. 2 we present the influence of a coupling to spin fluctuations in the normal state. It shows an intensity plot of the calculated spectral function $A(\epsilon, \boldsymbol{k})$ along a cut in the 1st Brillouin zone. The band maxima and minima as well as the Fermi velocity align very well with experimentally observed values [21]. By choosing the coupling constant g to be the same for all orbitals the band curvature becomes strongly enhanced leading to the observed shallow electron pocket at the X point. The bands are clearly renormalized by a factor of 1.5–2 and the quasiparticle width increases with energy. Thus, coupling to spin fluctuations gives an essential contribution to the above mentioned renormalization.

Superconducting order.—Our model is restricted to the low-energy region in the spin excitation spectrum, and does not precisely treat the incoherent high-energy part. However, this part considerably contributes to pairing [23], whereas the energy range of interest ($|\omega| < \omega_c =$ 200 meV) gives only a partial contribution (about 40%–50%) to the value of the superconducting order parameter. Thus, we add in our theory a contribution $\Delta_{\boldsymbol{k}}$ to the order parameter that results from the incoherent high-energy part of the spin-fluctuation spectrum. The order parameter is chosen to have $s^{\pm}$ symmetry, $\Delta_{\boldsymbol{k}}(T) = \Delta_0(T)\cos(k_x)\cos(k_y)$. This pairing state is supported by experiment
as well as numerical calculations [9,10,18,20,24]. The magnitude of the superconducting gap was observed to be $\bar{\Delta}(15\ \mathrm{K}) \approx 12$ meV at the inner holelike pocket as well as the corresponding nested pockets [9,10]. We choose Δ_0 so that the renormalized gap reaches the experimentally observed value at these particular points in the Brillouin zone, which gives $\Delta_0(0) = 18.1$ meV. Since detailed data for the temperature dependence is lacking, we assume $\Delta_0(T) = \Delta_0(0)\sqrt{1 - T/T_c}$.

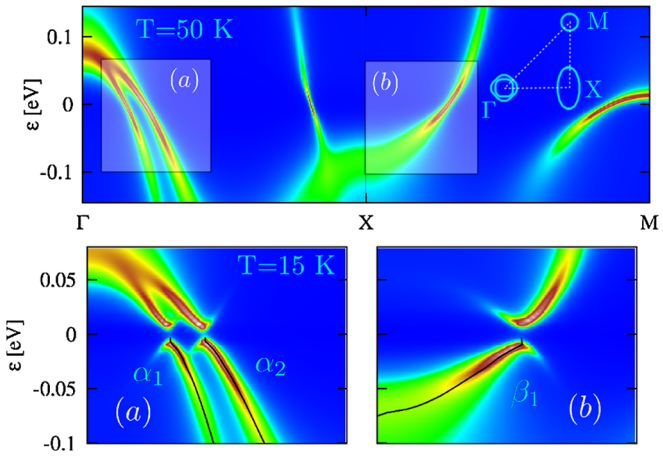

FIG. 2 (color online). On top: spectral function in the normal state for $T = 50$ K along a cut in the 1st Brillouin zone for $k_z = 0$. At bottom: the same for the superconducting state at $T = 15$ K for the square regions indicated (a) and (b) in the top panel. The black lines show MDC-derived dispersions for the (a) α_1 and α_2 band and the (b) β_1 band.

Dispersion and linewidth.—In the superconducting state, the dispersions shown in the upper panel of Fig. 2 are modified due to the appearance of the superconducting gap on the one hand, and the modifications of the spin excitation spectrum that is coupled to the conduction electrons on the other hand. In the lower panel of Fig. 2 extracts from the holelike and electronlike pockets at the Γ and X point are presented for 15 K. At first glance the intensity plots show no clear hint of the bosonic resonance, in contrast to the eye-catching break features in the cuprates [25]. In order to extract a quantitative effect we need to analyze differences between the dispersions and linewidths in the normal and superconducting state in detail.

Since multiple orbitals need to be taken into account in the case of pnictides, the linewidth function and the renormalization of the dispersion cannot be related in an easy way to theoretically obtained self-energies. For this reason we extract quantities from theoretically obtained spectral functions exactly as they are extracted in ARPES experiments [14,15]. For fixed energy the momentum dependence of the spectral function (called momentum distribution curve, or MDC) is peaked, with the peak often well approximated by a Lorentzian [see inset of Fig. 3(b)]. If the self-energy does not vary much as a function of momentum over the width of such an MDC peak, the MDC spectral function is of the form

$$A_\epsilon(\boldsymbol{k}) = \frac{1}{\pi}\,\frac{\Sigma''_{\epsilon,k_\epsilon}}{\{\boldsymbol{v}_\epsilon(\boldsymbol{k} - \boldsymbol{k}_\epsilon)\}^2 + \{\Sigma''_{\epsilon,k_\epsilon}\}^2}, \tag{3}$$

where $\boldsymbol{k}_\epsilon$ determines the maximum point of the MDC, and $\boldsymbol{v}_\epsilon = (\partial\boldsymbol{k}_\epsilon/\partial\epsilon)^{-1}$ [26]. In the bottom panel of Fig. 2 we show the MDC-derived dispersions $\epsilon = \varepsilon_{\boldsymbol{k}}$ obtained from $\boldsymbol{k}_\epsilon$ of the $\alpha_{1,2}$ and the β_1 band as black curves. The modification of the bare dispersion $\xi_{\boldsymbol{k}}$ to $\varepsilon_{\boldsymbol{k}}$ can be expressed in terms of the real part of an *effective* self-energy, Σ', that is defined by $\varepsilon_{\boldsymbol{k}} = \xi_{\boldsymbol{k}} + \Sigma'(\varepsilon_{\boldsymbol{k}}, \boldsymbol{k})$. The bare dispersion is not measurable. However, as it is temperature independent, any *changes* of $\Sigma'(\varepsilon_{\boldsymbol{k}}, \boldsymbol{k}) \equiv \Sigma'_{\boldsymbol{k}}$ with temperature can be extracted experimentally by taking the

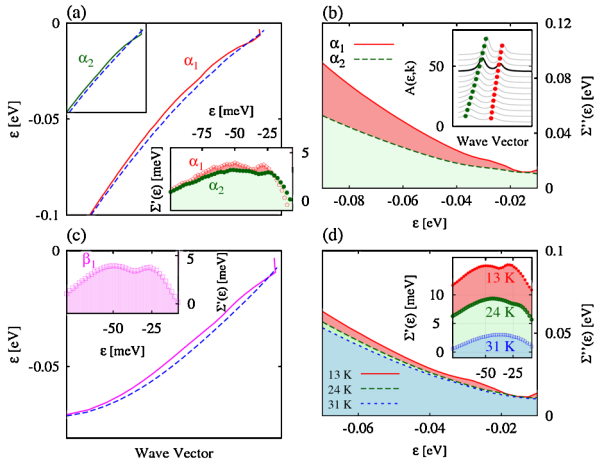

FIG. 3 (color online). (a) and (c) MDC-derived dispersions at the α_1, α_2 and β_1 band at $T = 15$ K (solid) and $T = 50$ K (dashed). The insets show the real part of the effective self-energy $\Sigma'(\epsilon) = \Sigma'_{\epsilon,k_\epsilon}$. (b) Imaginary part of the effective self-energy at $T = 15$ K at the α_1 (solid) and the α_2 (dashed) band. (d) Temperature dependence of the imaginary effective self-energy at the α_1 band and the real part at the β_1 band.

difference between two MDC-derived dispersions at fixed $\boldsymbol{k}$. Hence the influence of the resonance can then be quantified using the relation $\Sigma'^{T}_{\boldsymbol{k}} - \Sigma'^{T_{\mathrm{ref}}}_{\boldsymbol{k}} = \varepsilon^{T}_{\boldsymbol{k}} - \varepsilon^{T_{\mathrm{ref}}}_{\boldsymbol{k}}$ with a given reference temperature T_{ref} well inside the normal phase.

In Figs. 3(a) and 3(c) the MDC-derived dispersions of the $\alpha_{1,2}$ and the β_1 band in the normal at $T_{\mathrm{ref}} = 50$ K and superconducting state at $T = 15$ K are shown. The real part of the effective self-energies in the respective inset features a broad maximum at ≈ 50 meV as well as a peak at lower energies. This peak appears due to coupling to the resonance at energy $\Delta^{\varrho} + \Omega^{T}_{\mathrm{res}}$, where Δ^{ϱ} is the gap at the corresponding Fermi surfaces that are nested by an antiferromagnetic wave vector.

In Fig. 3(b) we discuss the imaginary part of the effective self-energy, $\Sigma''(\epsilon) \equiv \Sigma''_{\epsilon,k_\epsilon}$, that determines the linewidth of the MDC. Assuming that it weakly depends on momentum in a small region around k_ϵ it is given by $\Sigma''_{\epsilon,k} \approx \boldsymbol{v}_\epsilon \delta\boldsymbol{k}_\epsilon$, and $|\delta\boldsymbol{k}_\epsilon|$ is the full width at half maximum (FWHM) of the Lorentzian in reciprocal space in direction of $\boldsymbol{v}_\epsilon$. As seen in the figure it exhibits a linear dependence for higher energies, i.e., $\Sigma''(\epsilon) \propto |\epsilon|$, consistent with marginal Fermi liquid theory [27]. This results from the coupling to the continuum, in particular, from the slow decay of the spin-fluctuation spectrum towards high energies. The spin resonance leads to a weak hump feature in $\Sigma''(\epsilon)$ for excitation energies between 20–30 meV at the α_1 band, which is apparently observed in experiment [15]. When decreasing the temperature below T_c the resonance signature in the self-energies follows the temperature dependence of the resonance, as shown by selected examples in Fig. 3(d). We note that the correct magnitude of the linear in ϵ high-energy part of $\Sigma''(\epsilon)$ restricts the coupling strength $g^2\chi_0$. The experimental observations [15] are reproduced with a coupling strength $g^2\chi_0 = 1.17 \times 10^3\ \mu_B^2\,\mathrm{eV\,K}$. With this, all parameters of the theory are fixed by the high-energy behavior of the electronic spectra, and consequently all low-energy features discussed above are true predictions of the theory.

Conclusions.—We have shown that coupling to spin-excitations can quantitatively account for the renormalization of quasiparticle dispersions in both the normal and superconducting state of $Ba_{1-x}K_xFe_2As_2$ and likely also of other compounds with comparable properties. Given an experimental value of χ_0, it is possible to extract the spin-fluctuation coupling constant g. This value is not known for $Ba_{1-x}K_xFe_2As_2$, but was found to be $\chi_0 = (3.8 \pm 1.0) \times 10^4\ \mu_B^2\,\mathrm{eV}^{-1}\,\mathrm{K}$ for optimally doped $BaFe_{1.85}Co_{0.15}As_2$ [7]. Inserting this value, we infer $g \approx 0.15$–0.2 eV from our calculation. This coupling strength is large enough to imply a dominantly magnetic pairing scenario in the iron-pnictide superconductors.

We would like to thank S. Graser, J. Cole, and G. Schön for helpful discussions.

[1] Y. Kamihara *et al.*, J. Am. Chem. Soc. **130**, 3296 (2008).
[2] I. I. Mazin *et al.*, Phys. Rev. Lett. **101**, 057003 (2008).
[3] V. Cvetkovic and Z. Tesanovic, Europhys. Lett. **85**, 37002 (2009); arXiv:0804.4678.
[4] L. Boeri, O. V. Dolgov, and A. A. Golubov, Phys. Rev. Lett. **101**, 026403 (2008).
[5] J. Zhao *et al.*, Nature Mater. **7**, 953 (2008).
[6] S. Nandi *et al.*, Phys. Rev. Lett. **104**, 057006 (2010).
[7] D. S. Inosov *et al.*, Nature Phys. **6**, 178 (2009).
[8] A. D. Christianson *et al.*, Nature (London) **456**, 930 (2008).
[9] H. Ding *et al.*, Europhys. Lett. **83**, 47 001 (2008).
[10] K. Nakayama *et al.*, Europhys. Lett. **85**, 67 002 (2009).
[11] I. I. Mazin and J. Schmalian, arXiv:0901.4790.
[12] D. Parker *et al.*, Phys. Rev. B **78**, 134524 (2008); A. V. Chubukov, D. V. Efremov, and I. Eremin, Phys. Rev. B **78**, 134512 (2008); T. A. Maier and D. J. Scalapino, Phys. Rev. B **78**, 020514 (2008).
[13] M. Eschrig, Adv. Phys. **55**, 47 (2006).
[14] L. Wray *et al.*, Phys. Rev. B **78**, 184508 (2008).
[15] P. Richard *et al.*, Phys. Rev. Lett. **102**, 047003 (2009).
[16] See supplemental material at http://link.aps.org/supplemental/10.1103/PhysRevLett.106.047003.
[17] M. D. Lumsden *et al.*, Phys. Rev. Lett. **102**, 107005 (2009); J. T. Park *et al.*, Phys. Rev. B **82**, 134503 (2010).
[18] S. Graser *et al.*, Phys. Rev. B **81**, 214503 (2010).
[19] T. D. Stanescu, V. Galitski, and S. Das Sarma, Phys. Rev. B **78**, 195114 (2008).
[20] S. Graser *et al.*, New J. Phys. **11**, 025016 (2009).
[21] H. Ding *et al.*, arXiv:0812.0534.
[22] D. H. Lu *et al.*, Physica (Amsterdam) **469C**, 452 (2009); Y. Sekiba *et al.*, New J. Phys. **11**, 025020 (2009).
[23] J. Zhang *et al.*, Phys. Rev. B **82**, 134527 (2010).
[24] R. Thomale *et al.*, Phys. Rev. B **80**, 180505(R) (2009).
[25] A. Kaminski *et al.*, Phys. Rev. Lett. **86**, 1070 (2001).
[26] M. R. Norman *et al.*, Phys. Rev. B **64**, 184508 (2001).
[27] P. B. Littlewood and C. M. Varma, Phys. Rev. B **46**, 405 (1992).